Particle and Impurity Transport in Electron-Heated Discharges in TCV

A. Zabolotsky[1], M. Bernard[1], A. Bortolon[1], B.P. Duval[1] , E. Fable[1],
A. Karpushov[1], M. Maslov[1], O. Sauter[1], V. Piffl[2], Ch. Schlatter[1],
G. Veres[3], H. Weisen[1]

[1)]*Ecole Polytechnique Federale de Lausanne, Centre de Recherches en Physique des Plasmas Association EURATOM - Confederation Suisse, 1015 Lausanne, Switzerland*
[2)]*Institute of Plasma Physics, Czech Academy of Sciences, Prague, Czech Republic*
[3)]*KFKI-Research Institute for Particle and Nuclear Physics, Budapest, Hungary*

Abstract: The behaviour of particle and impurity density profiles in electron heated Ohmic, ECH and ECCD L-modes and H-modes as well as eITB's is investigated in view of developing physics understanding for a predictive capability for a-heated, ignited reactor conditions. Experimental observations in stationary L - modes show that density peaking depends mainly on the edge safety factor. Additional electron heating generally leads to a broadening of the density profiles and appearance of dependence on the power ant it's deposition location. The dominant edge safety factor dependence observed is supportive of turbulent equipartition (TEP) theory, which predicts inward convection in the presence of turbulence. On the other hand, the correlation of the density peaking with temperature gradients in eITB regimes points out to the dominance of the turbulence of thermodiffusive type. Carbon profiles in L-mode discharges is found to be peaked with anomalous transport coefficients.

Introduction

The transport of particles in magnetically confined plasmas has important implications on fusion performance. On the positive side is a potential boost in fusion power output if fuel density profiles profiles are peaked. On the downside an increased proneness to impurity accumulation and difficulty of removing of He ash produced by fusion reactions.

Recently the study of particle transport in tokamaks has made important progress, providing a fairly consistent picture of its behaviour in several devices and uncovering differences in the behaviour of L-mode and H-mode, allowing for a tentative prediction for ITER [1-3]. Studies performed in TCV Ohmic and in JET L-mode LHCD heated discharges have shown that the electron density peaking depends on the current profile peaking [2,3]. In the presence of additional core heating, results from ASDEX Upgrade [4] show a partial flattening of the density profiles. In this paper we present a summary of TCV results on experimentally observed parameter dependencies distinctive for TCV Ohmic and EC heated L and H - modes as well as discharges with an electron internal transport barrier.

The TCV (R_0=0.88 m, a<0.25 m, B_T<1.5 T, I_p<1.1 MA) ECRH system includes six gyrotrons for heating at the second harmonic of the electron cyclotron resonance [5]. Operating at 82.7 GHz, these microwave sources can deliver up to 2.7 MW to the plasma for a maximum pulse length of 2 seconds. Three recently installed 118GHz gyrotrons for 3rd harmonic (X3) heating, with about 1.5MW of total power, can be used at high densities, above X2 cut-off, typical for H - mode discharges.

The results presented are based on an extensive analysis of databases containing about 2000 electron density profiles and transport relevant plasma parameters taken in stationary phases of Ohmic and ECRH discharges [6 - 8]. The databases cover a wide parameter range, $0.9\cdot10^{19} \le n_e(0) \le 3\cdot10^{19}$ m^{-3}, $0.02\le\nu^*_{75}\le1$, $1.2 \le \kappa_a \le 2.3$, $3 \le q_{95} \le 20$, $-0.65\le\delta\le0.6$, where $n_e(0)$ is the central electron density, ν^*_{75} is the ratio of pitch angle scattering frequency to the banana

trajectory bounce frequency calculated at 75% of poloidal flux, k_a and δ are the elongation and triangularity at the plasma edge, q_{95} safety factor measured at 95% of the poloidal flux.
A profile peaking factor $f_{e0} / < f_e >$, where f_{e0} is the central value of quantity f, and < > denotes volume average, is often chosen as a quantifier for the density profils peakedness. In order to reduce the scatter due to random sampling with respect to the sawtooth cycle, we introduce a "clipped" density peaking factor defined as $n_{e1} / < n_e >$ where n_{e1} is the electron density at the sawtooth inversion radius, $n_e = n_{e1}$ for $\rho < \rho_{inv}$ and $n_e = n_e$ for $\rho > \rho_{inv}$. This "clipped" profile is representative of flattened profile just after the sawtooth crash. In the absence of sawtooth oscillations, the "clipped" peaking factor is equivalent to the traditional peaking factor $n_{e0} / < n_e >$.

Density profile peaking

It is widely accepted that peaked electron density profiles in tokamak plasmas result from an inward particle pinch. To explain peaked density profile behaviour, three pinch mechanisms, turbulent thermodiffusion (TTD) [9], turbulent equipartition (TEP) [10] and the neoclassical Ware pinch [11] are usually considered. The former two are predicted to result from electrostatic drift wave turbulence due to unstable trapped electron (TEM) and ion temperature gradient modes (ITG).
The density gradient in steady state may be written in the following form:

$$\frac{\nabla n}{n} = \frac{1}{D}\left(\frac{\Gamma_{source}}{n} + V_{ware} + C_{Te}\frac{\nabla T}{T} - C_q \frac{\nabla q}{q} \right) \quad (1)$$

where D is a diffusion coefficient (anomalous and neoclassical), Γ_{source} is the flux associated with the particle source, V_{ware} is the neoclassical Ware pinch, C_{Te} is the termodiffusion coefficient, C_q is the turbulent equipartition (TEP) term coefficient. The coefficient C_q is positive, whilst C_{Te} may be either positive or negative depending on the conditions (ITG or TEM) [12, 13]. The source is provided by the penetration of edge neutral particles to the core by a sequence of charge exchange events.
Fully ECCD sustained discharges in TCV have shown that peaked density profiles subsist in the absence of the Ware pinch [2]. Similarly, discharges in helium plasmas, where neutral penetration by successive charge exchange reactions is quenched because of the low cross section for double charge exchange, show that peaked density profiles are still observed in the absence of a core particle source [14]. The combination of these two observations provides experimental proof that peaked density profiles can only be explained by anomalous processes. Neutral penetration calculation using the KN1D and DOUBLE-TCV codes have confirmed that the experimental density profiles are too peaked, even in deuterium plasmas, to be explained by edge fuelling and diffusive particle transport alone [14].

Particle transport in L -mode plasmas

The density peaking factor $n_{e1} / < n_e >$ in TCV L-mode Ohmic discharges was found to scale with the parameter $< j > /(j_0 q_0)$ [2]:

$$\frac{n_{e1}}{< n_e >} \approx \frac{1}{< j > /(j_0 q_0) + 0.22} \quad (2)$$

The parameter $< j > /(j_0 q_0)$ where <j> is the cross-sectional average toroidal current, j_0 and q_0 the plasma current density and the central safety factor at the magnetic axis respectively, represents a generalization to arbitrary cross sections of the edge safety factor $1/q_a$. This

parameter was also found to provide a good scaling parameter for Ohmic sawtooth inversion radii, temperature and pressure profiles [15,16]. Fig 1 shows that density peaking in ECRH L-

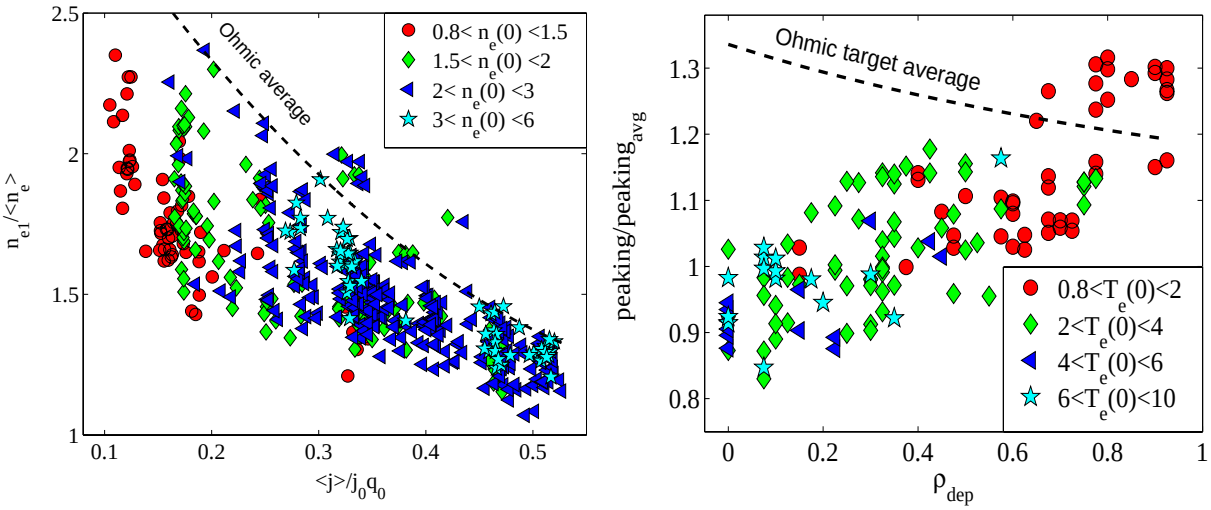

Fig. 1 ***A)*** *Scaling of electron density peaking in ECRH discharges with edge safety factor <j>/(j₀q₀). The average density peaking in Ohmic discharges from Eq. 2 is plotted as a dashed line. Symbols separate classes of central densities (10^{19} m^{-3}). ECRH power in the dataset is higher than 0.45 MW.* ***B)*** *Scaling of the parameter peaking/peaking$_{avg}$ with ρ_{dep} (see definitions of ρ_{dep} in the text) in ECRH discharges presented on* ***A****. Symbols refer to the classes of the central temperatures in keV.*

mode discharge also depends on $< j > /(j_0 q_0)$ with clear effect of profile broadening as a result of additional heating. At fixed $< j > /(j_0 q_0)$ the peaking can be as low as 60% of the peaking in the Ohmic target discharge.

Significant vertical scatter of the data at fixed $< j > /(j_0 q_0)$, which is well beyond the errors, estimated to be less than 15%, indicates that in ECRH discharges, $< j > /(j_0 q_0)$ is no longer the only scaling parameter as in the Ohmic case. We performed an extensive regression study of the density peaking dependences in ECRH discharges on parameters such as the loop voltage $V_{LOOP} = 2\pi R_0 E_{\|}$ ($E_{||}$ is parallel electric field and R_0 is the major radius), the volume average density $<n_e>$, the effective collisionality (which determines the drift mode growth rate) at 75% of the square root of poloidal flux $\nu_{eff\,75} = \nu_{ei} / \omega_{De} \approx 10^{-14} R_0 T_e^{-2} n_e Z_{eff}$ (where ω_{De} is the curvature drift frequency [12], R_0 is the major radius and Z_{eff} is the effective charge), the inverse temperature "clipped" peaking factor $< T_e > / T_{e1}$ and the total ECRH power P_{ECRH}. Among the parameters tested using two parameter linear regressions, none was found to provide a statistically meaningful alternative to

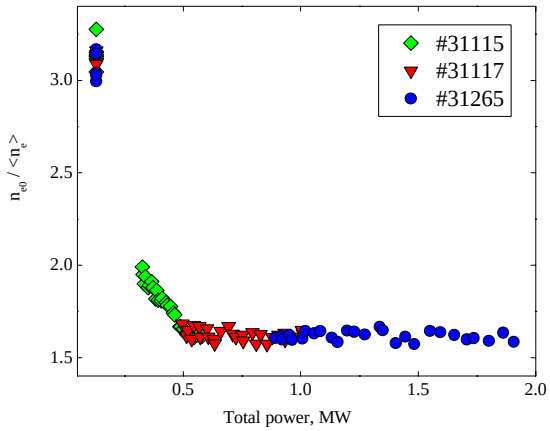

Fig. 2 *Dependence of the density peaking factor on the absolute value of ECRH power in three discharges with the same target plasma (I_p~0.11 MA, q_{95}~8, Ohmic power of 0.13 MW) and the same power deposition location*

$< j > /(j_0 q_0)$. The study using three parameter regression (one parameter in addition to $< j > /(j_0 q_0)$) revealed a dependence of $n_{e0} / < n_e >$ on the power deposition location defined as the position of the maximum of the power deposition profile. This dependence on ρ_{dep} is illustrated on Fig 1B. We used the quantity peaking/peaking$_{avg}$ obtained by division of the density peaking by the average density peaking from Eq. 1 and which scales out the dependence of $n_{e1} / < n_e >$ on $< j > /(j_0 q_0)$. The peaking/peaking$_{avg}$ parameter decreases when deposition becomes more central, depending almost linearly on ρ_{dep}. The lowest peaking in ECRH L-mode discharges is observed for on-axis deposition. At the same time, for far off-axis heating, the peaking can be slightly higher than the average Ohmic peaking, although the quality of the data does not allow to unambiguously prove this surplus of peakedness. Based on the results of the regression study, the density peaking dependence in the case of EC heating with additional power higher than 0.45 MW (at least one gyrotron at full power) can be expressed as:

$$\frac{n_{e1}}{< n_e >} \approx \frac{1}{0.9 < j > /(j_0 q_0) - 0.2 \rho_{dep} + 0.44} \qquad (3)$$

The details of the transition from peaked Ohmic to flatter profile during ECRH was revealed in a series of power scans in L-mode with additional power changing from 0.18 MW to 2 MW at fixed deposition location (ρ_{dep}~0.35) at constant plasma current 0.11 MA, corresponding to q_{95}~8, constant shape and density. At such high q_{95}, MHD activity such as m=1, n=1 modes and sawteeth are absent. In each of the discharges power was gradually ramped up during the 1s heating pulse. The resulting dependence of the density peaking factor on the injected ECRH power is shown on Fig 2. A strong dependence of the density peaking on the ECRH power below 0.5 MW is followed by resilient behaviour in response to a further increase of the heating power. The final level of the peaking depends on the deposition location (see Eq 3). Although core flattening by ECH is in qualitative agreement with drift wave turbulence theory, this saturation is not predicted by theory.

Particle transport in H -mode plasmas

The evidence of peaked electron density profiles in JET and ASDEX H-modes was shown in Refs. [3, 4]. However the dominance of neutral beam heating on these devices does not allow to extrapolate these results to the case of alpha heating in a fusion reactor.

Density peaking in purely electron heated TCV Ohmic H-mode was found to be similar to the peaking in L-mode [2]. EC heated H-modes with $\beta_N \sim 2$ and $T_e / T_i \sim 2$ have recently been obtained on TCV using 3rd harmonic ECRH [17]. 1.35 MW X3 heating power applied to Ohmic H - modes raises the central electron temperature from 0.8 to 2.4 keV and usually causes a change of ELM type from relatively small ELMs to giant ones. The density profile during ECRH flattens modestly in the presence of giant ELMs (see Fig 3) and remains the same as in the Ohmic target for ELM-free shots [7]. Due to pure electron heating, TCV has a very low electron-ion coupling in comparison to JET or ASDEX and therefore high T_e / T_i ratio. This is a very favourable condition for TEM destabilizing however even in this case only moderate flattening is

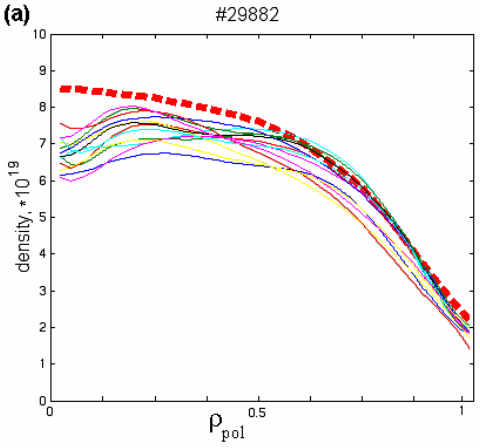

***Fig. 3** Multiple TS measurements of density profiles during X3 heating for ELMy phase. Red dashed line – density profile in an Ohmic H-mode plasma*

observed. Therefore flattening of the ITER density profile as a result of the dominant alpha heating is expected to be even less pronounced than in TCV ECRH H-mode.

Particle transport in eITB

Amongst the possible approaches to magnetic confinement fusion, the so-called advanced Tokamak operational scenarios feature the possibility of creating and sustaining an internal transport barrier (ITB) [18]. In ITB discharges, the low (or negative) shear is believed to suppress the turbulence in the plasma core, leading to reduced transport and to the formation of a transport barrier characterized by steep localized temperature and density gradients. eITB discharges can be characterised [19] by their confinement enhancment factor $H_{RLW} = \tau_e / \tau_{RLW}$, where τ_e is the electron energy confinement time and τ_{RLW} is confinement time predicted by the semi-empirical Rebut-Lallia-Watkins scaling [20]. The presence of strong eITB's ($H_{RLW} > 3$ for TCV) involves a significant reversal of the central magnetic shear.

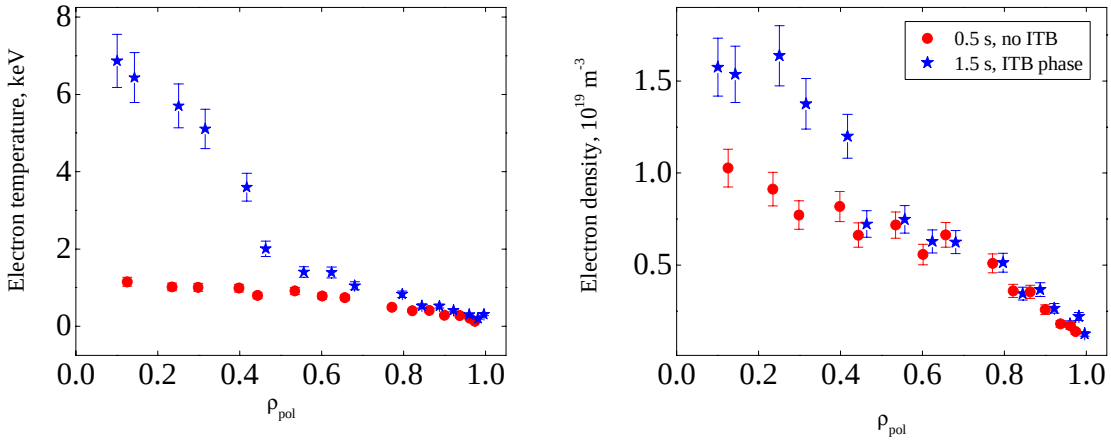

***Fig. 4** Profiles of the electron temperature and the electron density in the discharge with eITB #26033*

Fig. 4 shows an example of density and temperature profiles in a discharge with a plasma current I_p = 0.11 MA in which the combined effect of on-axis ECH and off axis co-ECCD (1.3 MW) created an eITB at ρ_{pol} ~ 0.5 with H_{RLW} ~ 3.5. A local change of ∇T_e from ρ_{pol} ~ 0.5 during the eITB phase of the discharge is clearly observed. A local change of the gradient, with increased profile peakedness, although less pronounced, is observed on the electron density profile. Once the eITB is formed, the gradients of the density profiles inside the barrier remain constant for the whole duration of the power pulse, typically over 500 energy confinement times (limited only by a length of gyrotron pulse ~ 2 s).

The density peaking during strong eITB departs from the general scaling for ECRH discharges. As seen from Fig. 5A, discharges with eITB's are more peaked even than Ohmic target discharges, reaching $n_{e1} / < n_e >$ ~ 3.5 in extreme cases. All the points on this scaling which have strong eITB's, are located in the low current region because of the limitation of the TCV current drive system to produce strong reversal of the shear at high plasma current.

The density peaking in strong eITB discharges becomes independent of current profile peakedness. At the same time temperature gradients start to be important. Fig. 5B [8] shows the relation between the ratio and normalized gradient of electron temperature. At low values of H_{RLW}, which corresponds to the L-mode, temperature and electron density profile are not correlated. At large R/L_{Te} observed in strong eITBs, the profiles of electron density are such that $R/L_{ne} \approx (0.4 \div 0.5) R/L_{Te}$, independently of other plasma parameters (within the error

bars), which implies the existence of a dominantly inward pinch of `thermodiffusive' type, due to the direct R/L_{Te} proportionality. In these discharges, since the core magnetic shear s is weak or negative, a strong stabilization of turbulence is expected. In particular, it has been shown that the main active microinstability is the trapped electron mode (TEM) [21] and that it is stabilized by reverse shear profiles in this type of scenarios.

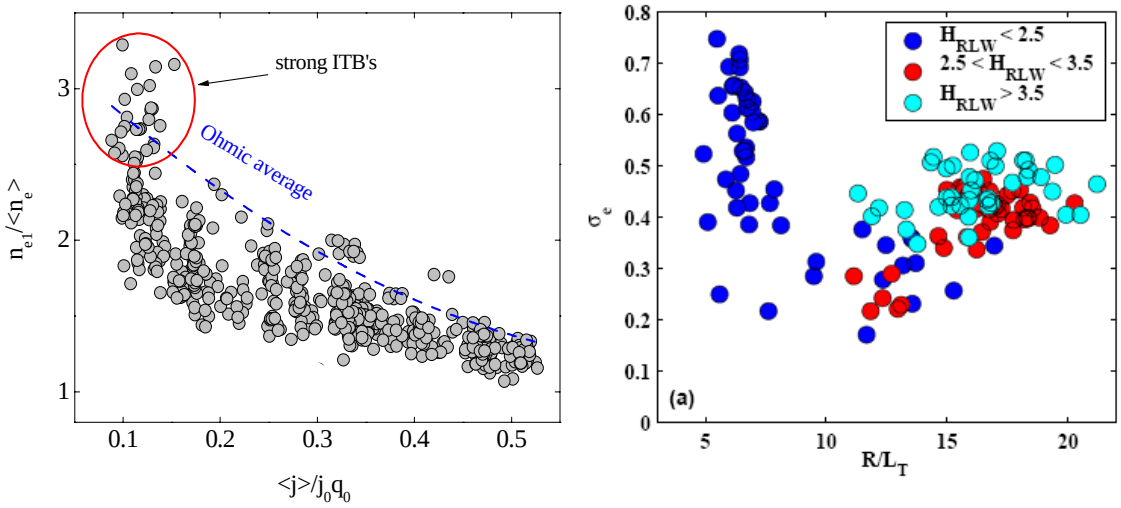

***Fig. 5** A) Scaling of the density peaking with $< j > /(j_0 q_0)$. B) $\sigma_e = L_n / L_T$ vs R/L_T shown for different H_{RLW} factors*

It was also found that the link between ∇n_e and ∇T_e is conserved when the q profile inside the barrier is modified by small current perturbations [22, 23]. As a result, the density profile in eITBs does not depend directly on the q profile, contrary to the L-mode. It is interesting to note that a similar result, $\nabla n_e = 0.5 \cdot n_e \nabla T_e / T_e$, has been obtained in the context of a study of the edge transport barrier properties in ASDEX Upgrade [24]. This could mean that there is a more general relation between heat and particle transport in transport barriers.
Argon puff experiments have revealed distinct changes in impurity confinement in the barrier region, apparent as differences in time scales for the density evolution outside and inside the barrier [25]. The transport coefficients inside the barrier at the position of maximum of the normalized gradients were estimated to be D_{ITB}~0.5 m^2/s and V_{ITB} ~ 1 m/s which is lower that D and V in L - mode in the same region (D_L~1 m^2/s, V_L ~ 3 m/s) and still significantly higher than the neoclassical transport level (D_{neo} ~ 0.02 m^2/s).

Cross-field transport of intrinsic carbon impurities

The steady-state radial profiles of fully ionized carbon released from TCV wall tiles were measured using an active Charge eXchange Recombination Spectroscopy (CXRS) diagnostic. The line emission from fully ionized carbon C^6 (transition 8-7, 529.1 nm) was used to obtain the density of C^{6+} at 8 radial locations [26].
Fig. 3A shows an example of C^{6+} profile measured in an low current Ohmic L-mode discharge. In this particular case, the normalized profile of C^{6+} is more peaked than the electron density profile. A general dependence of the normalized gradient ($\nabla f / f$) at ρ_{pol}=0.5 for C^{6+} and for the electron density on the parameter $<j>/j_0q_0$ is shown on Fig. 6B. In general, for low current Ohmic discharges the C^{6+} profiles are more peaked than the electron density profiles and for the high current discharges (q_{95}<4) the normalized gradients of C^{6+} and of n_e become similar. This scaling of normalized C^{6+} gradients does not depend on the absolute value of the electron density or temperature.

To obtain the carbon transport coefficients from measured C^{6+} profile, as well as the profile of the total carbon density, the 1D impurity transport code STRAHL was used [27]. Such modeling work uses assumed profiles of D and V as a function of ρ as input and provides a normalized profile of C^{6+} as an output. For D parabolic profiles were chosen and the best fitting profile of V was found from an independent scan with V specified at 5 nodal points. Attempts to model the observed profiles without a pinch failed, unless the impurity diffusion coefficients were assumed to be significantly higher than the heat diffusivities and the modeled diffusion coefficients of laser ablated silicon in similar experiments. Carbon confinement times of the order of 20 ms (comparable with τ_e and Si confinement times) were therefore assumed in order to constrain the absolute values of D [28, 29]. These simulations show that the experimental profiles of C^{6+} and assumed carbon confinement time are reproduced only if an inward pinch is present. The best fitting diffusion coefficients are clearly anomalous both in low and high current Ohmic discharges. The best fitting inward pinch velocity is clearly anomalous only in low current discharges and approaches the neoclassical level at high current, although it is still anomalous. With the best fitting D and V, the concentrations of partly ionized stages of carbon are found to be negligible at ρ_{pol}=0.5, therefore the scaling presented on Fig. 6B is valid for total C profile.

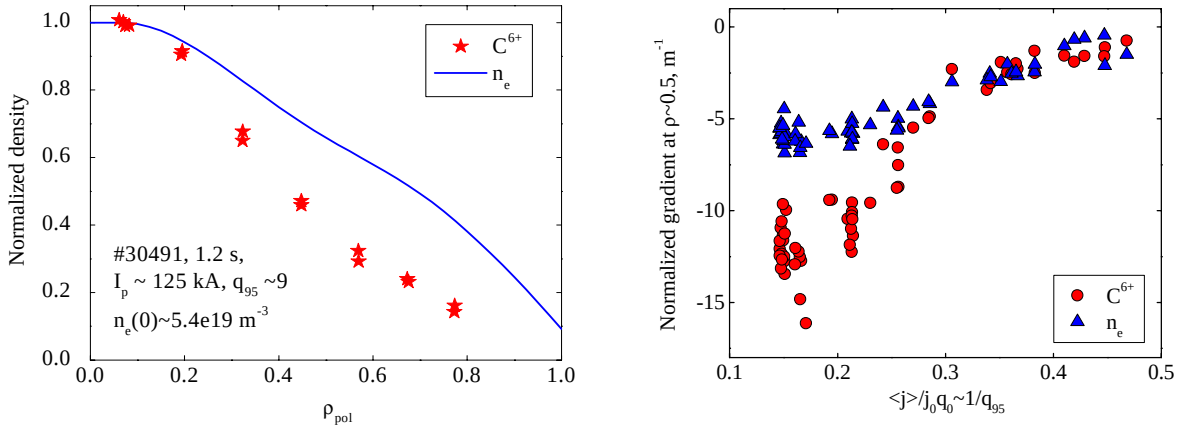

Fig. 3 A) *Normalized profiles of C^{6+} measured by CXRS (stars) and of electron density profiles in L-mode Ohmic discharge.* ***B)*** *Normalized gradients of C^{6+} measured by CXRS and density profiles fit from TS at ρ_{pol} = 0.5*

Conclusions

Moderately peaked electron density profiles are observed in virtually all plasma conditions in TCV. There is a clear difference in the particle transport, between L-mode discharges and eITB discharges. In L-mode discharges density peaking depends mainly on current profiles whereas in the regions of strong eITB density profile are coupled with electron temperature profiles. This apparent contradiction is consistent with the drastic change in the type of the expected turbulence because of the completely different q profile and associated magnetic shear. A direct proportionality between R/L_n and R/L_T in eITB's indicates a dominance of thermodiffusive type of turbulent pinch. In contrast, in L-mode discharges the scaling of the density peaking with the width of the current profile is consistent with TEP. Measurements of steady state carbon profiles indicate that peaked density profiles in L-mode plasma are accompanied by peaked carbon profile resulting from anomalous transport, despite superficial similarities with neoclassical impurity peaking. In stationary purely electron heated TCV H-mode discharges with reactor relevant $\beta_N \sim 2$, a density peaking factor around 1.5 was observed.

The observations of peaked density profiles during pure electron heating suggest that even in the presence of strong alpha heating in a fusion reactor, the expected fusion power will be significantly higher that one predicted for the flat fuel profile .

Acknowledgement: This work was partly supported by the Swiss National Fund for Scientific Research.

References

[1] X. Garbet et al., Plasma Phys. Control. Fusion, vol. 46, 2004
[2] A. Zabolotsky et al., Plasma Physics and Controlled Fusion 45, No 5, 735-746, 2003
[3] H. Weisen et al., Nuclear Fusion vol. 45, L1-L4, 2005
[4] C. Angioni et al., Nucl. Fusion, vol. 44, p. 827, 2004
[5] T. P. Goodman et al., 1997 Fusion Technology: Proc. 19th Symp.on Fusion Technology Lisbon, vol 1, p 565, 1996
[6] A. Zabolotsky et al., Plasma Phys. Control. Fusion 48, p. 1, 2006
[7] M.Maslov et at. 33th EPS conference on Plasma Physics, (Rome 2006), O3.005
[8] E Fable et al., Plasma Phys. Control. Fusion 48 No 9, p. 1271, 2006
[9] F. Miskane and X. Garbet, Phys. Plasmas, vol. 7, p. 4197, 2000.
[10] J. Nycander and V. V. Yancov, Phys. Plasmas, vol. 2, p. 2874, 1995
[11] A. A. Ware, Phys. Rev. Lett., vol. 25, p. 916, 1970
[12] C. Angioni et al., Phys. Rev. Lett., vol. 90, p. 205003, 2003
[13] A. J. H. Nordman and J. Weiland, Nucl. Fusion, vol. 30, p. 983, 1990
[14] A. Zabolotsky et al., Nucl. Fusion 46, p. 594, 2006
[15] H. Weisen et al., Nucl. Fusion, vol. 42, p. 136, 2002
[16] H.Weisen and E. Minardi, Europhysics Letters, vol. 56, p. 542, 2001
[17] S. Alberti, et al, 2005 Nucl. Fusion 45 1224-1231
[18] R. C. Wolf, Plasma Phys. Contr. Fus. 45, R1-R91, 2003
[19] M. A. Henderson et al., Plasma Phys. Control. Fusion, vol. 46, 2004
[20] P. H. Rebut et al., Proc. 12th Int. Conf. on Plasma Physics and Controlled Nuclear Fusion Research, Nice 1988, IAEA Vienna, vol. 2, p. 191, 1989
[21] A. Bottino et al., Plasma Phys. Contr. Fus. 48 (2), 215-233 (2006)
[22] O. Sauter et al., Phys. Rev. Lett. 94, 105002 (2005)
[23] T. P. Goodman et al., Plasma Phys. Contr. Fus. 47 (12B), B107-B120 (2005)
[24] L. D. Horton et al., Nucl. Fus. 45, 856 (2005)
[25] E. Fable et al. in Theory of Fusion Plasmas, Proc. of the Joint Varenna-Lausanne Int. Workshop, Varenna, 2006 (Editrice Compositori, Bologna 2006)
[26] A. N. Karpushov et al., Fusion Eng. Des. 66–68 (2003), 899–904
[27] R.Dux. STRAHL User Manual, IPP Garching, Germany http://www.rzg.mpg.de/~rld/strahl.ps
[28] A.Zabolotsky et at. 33th EPS conference on Plasma Physics, (Rome 2006) 1.145
[29] E.Scavino et al., Plasma Phys. Control. Fusion 45 (2003) 1961